

Interesting magnetic response of the nuclear fuel material UO_2

Sudip Pal¹, L. S. Sharath Chandra², M. K. Chattopadhyay^{2,3}
and S. B. Roy¹

¹ UGC DAE Consortium for Scientific Research, University Campus
Khandwa Road, Indore 452001, India

² Free Electron Laser Utilization Laboratory, Raja Ramanna Centre for Advanced
Technology, Indore-452 013, India

³ Homi Bhabha National Institute, Training School Complex, Anushakti Nagar,
Mumbai 400 094, India

E-mail: sbroy@csr.res.in

Abstract. Magnetic response of uranium dioxide (UO_2) has been investigated through temperature and magnetic field dependent dc magnetization measurements. UO_2 is a paramagnet at room temperature. The magnetic susceptibility, however, deviates from Curie-Weiss (CW) like paramagnetic behavior below $T = 280$ K. Further down the temperature UO_2 undergoes phase transition to an antiferromagnetic state below $T_N = 30.6$ K. The zero field cooled (ZFC) and field cooled (FC) magnetizations exhibit some distinct thermomagnetic irreversibility below T_N . The temperature dependence of the FC magnetization is more like a ferromagnet, whereas ZFC magnetization exhibits distinct structures not usually observed in the antiferromagnets. In low applied magnetic field this thermomagnetic irreversibility in magnetization exists in a subtle way even in the paramagnetic regime above T_N up to a fairly high temperature, but vanishes in high applied magnetic fields. Deviation from CW law and irreversibility between ZFC and FC magnetization indicate that the paramagnetic state above T_N is not a trivial one. Magnetic response below T_N changes significantly with the increase in the applied magnetic field. Thermomagnetic irreversibility in magnetization initially increases with the increase in the strength of applied magnetic field, but then gets reduced in the high applied fields. A subtle signature of a magnetic field induced phase transition is also observed in the isothermal magnetic field variation of magnetization. All these experimental results highlight the non-trivial nature of the antiferromagnetic state in UO_2 .

1. Introduction

Uranium di-oxide (UO_2) is a well known nuclear fuel material and used worldwide in nuclear reactors for electrical power generation and research. UO_2 is also recognized as a Mott-Hubbard insulator [1, 2], and it promises other technological applications apart from a nuclear fuel [3, 4]. Thermal conductivity is very important for the removal of heat produced in a nuclear reactor by fission in the nuclear fuel materials. As a result thermal

properties of UO_2 particularly have drawn much attention over the years [1, 5, 6, 7, 8]. UO_2 crystallizes in face centred cubic (fcc) calcium fluorite structure ($Fm\bar{3}m$), in which U^{4+} ions are surrounded by eight O^{2-} ions forming a cube [9]. Therefore, the anisotropic thermal conductivity reported in this compound is rather unexpected and emphasizes on the relevance of spin-phonon coupling, which is associated with the magnetic state of the system [8]. The Mott insulating state in UO_2 further highlights the importance of strong electron-electron correlation in the system [2, 4]. Various techniques, including neutron scattering and nuclear magnetic resonance (NMR) have revealed a complex 3k-non-collinear antiferromagnetic (AFM) spin ordering below $T_N = 30.6$ K. The transition is first order in nature and is accompanied by a small lattice distortion, predominantly in the oxygen cage [10, 11, 12]. In cubic crystal field, the nine fold degenerate ($5f^2$, $J = 4$) state splits up with a 3-fold degenerate ground state, resulting into Jahn-Teller (JT) instability [13].

Spin-orbit coupling, Coulomb interaction, antiferromagnetic exchange interaction and JT distortion are of comparable strength in UO_2 . Below T_N , a quadrupoler ordering is established together with AFM spin ordering, facilitated by the interaction between cooperative JT distortion, antiferromagnetic exchange interaction and $5f$ quadrupoles [14, 15, 16, 17]. While, there is some understanding of the physical properties of UO_2 in the antiferromagnetic state below T_N , characteristics of the high temperature state are not quite clear. The nature of the high temperature state, although considered to be paramagnetic, is not so straightforward. Temperature dependence of thermal conductivity exhibits a minimum at T_N and a maximum around $T = 220$ K, which clearly highlight unusual physical state above T_N . Moreover, a positive magnetostriction has been observed above T_N , whereas magnetostriction is negative in the AFM state. Neutron scattering has provided evidence for dynamic JT distortion of the oxygen sublattice above T_N [18, 19, 20, 21]. Temperature dependence of elastic constant above T_N also exhibit unconventional behavior [11]. UO_2 has been reported to be showing some other interesting physical properties, such as piezomagnetism and magnetoelastic memory driven by spin-lattice interaction [9].

Here we present a detailed study of the temperature (T) and magnetic field (H) dependence of magnetization (M) in UO_2 . The results of our study highlight various hitherto unknown interesting aspects of the magnetic response of UO_2 . We show that below $T = 280$ K the low field magnetization or susceptibility deviates from standard Curie-Weiss paramagnetic behavior. Abrupt changes in both the zero field cooled (ZFC) and field cooled (FC) magnetization are observed at $T_N = 30.6$ K where UO_2 undergoes a phase transition to antiferromagnetic state along with distinct thermomagnetic irreversibility i.e. $M_{ZFC}(T) \neq M_{FC}(T)$ inside the antiferromagnetic state. The magnetic response in the antiferromagnetic state changes considerably with the increase in the applied magnetic field. The observed behaviour may be correlated to a magnetic field induced phase transition. The thermomagnetic irreversibility in the antiferromagnetic state continues to exist in the temperature range above T_N and below $T = 150$ K, but it gets suppressed completely at higher applied magnetic fields.

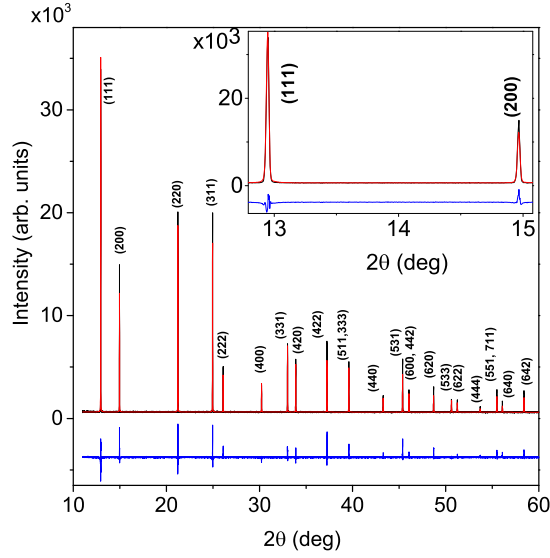


Figure 1. X-ray diffraction pattern of UO_2 powder sample recorded at room temperature using wavelength, $\lambda = 0.7121 \text{ \AA}$. The data have been fitted using rietveld refinement method. Indexes of the planes corresponding to peaks are also mentioned. The blue line at the bottom shows the difference between experimental data and fitted curve.

2. Experimental details

Powder sample of UO_2 has been prepared by reducing UO_3 in hydrogen atmosphere at 700°C at Bhabha Atomic Research Centre, Trombay. Room temperature X-ray diffraction data have been recorded at the wavelength of $\lambda = 0.7121 \text{ \AA}$ in the beamline-BL12 in Indus-2 synchrotron radiation source at Raja Ramanna Centre for Advanced technology (RRCAT), Indore, India. Magnetic measurements have been carried out in a MPMS-3 SQUID-VSM magnetometer (M/S Quantum Design, USA). Temperature dependence measurements of magnetization have been performed in temperature sweep mode of measurement at 0.5 K/min cooling and heating rate.

3. Results and discussion

Fig.1 shows the X-ray diffraction data of UO_2 measured at room temperature in $\theta - 2\theta$ geometry. In the inset, we have shown a magnified view of the data around (111) peak, which is the most intense peak in this case. Sharp diffraction peaks and flat background reveal the good crystalline nature of the sample. The data have been analyzed by Rietveld refinement method using Fullprof software package. All the peaks can be indexed in cubic fcc structure (space group $Fm\bar{3}m$), which rules out the presence of any secondary phase in the sample. The optimized lattice parameter obtained from fitting is, $a = 5.4594 \text{ \AA}$. Lattice parameter of UO_2 is sensitive to oxygen stoichiometry of the sample and follows an empirical law given by, $a = 5.4705 - 0.132x$, where x is defined as UO_{2+x} [22]. In our case, the obtained lattice parameter corresponds to, $x = 0.08$.

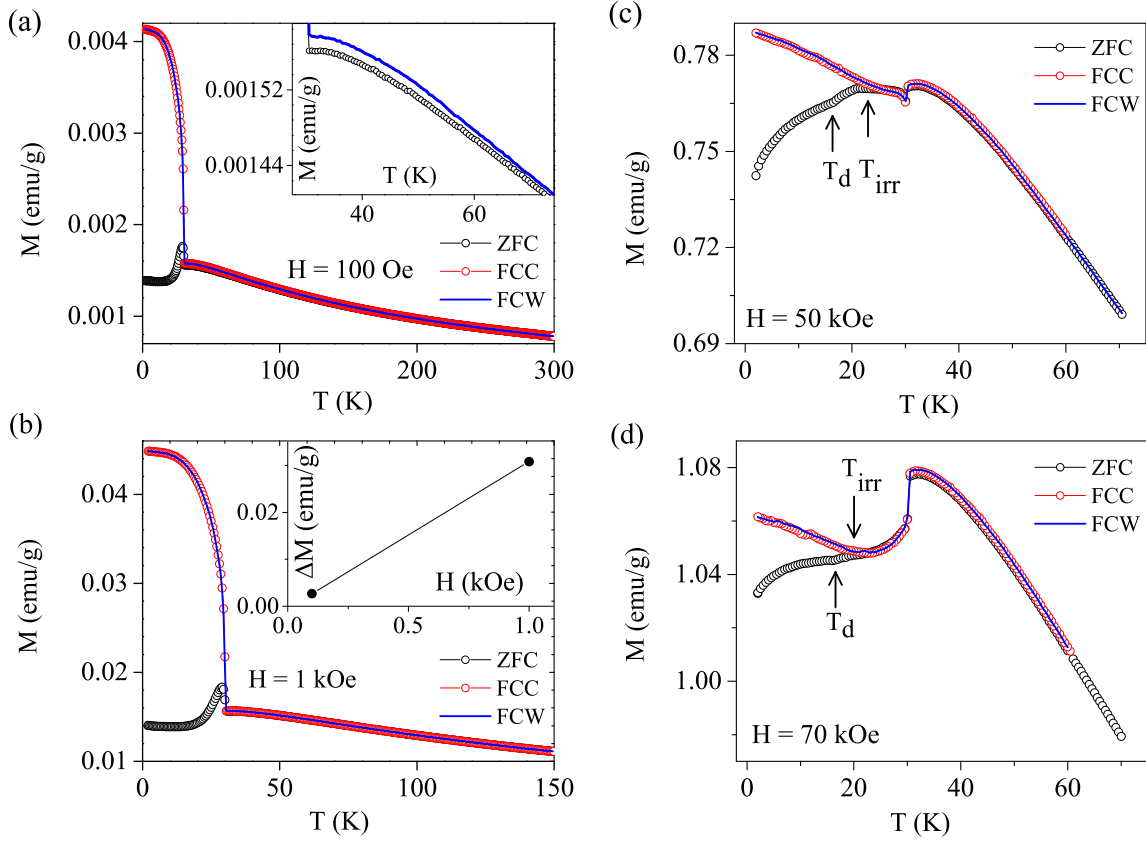


Figure 2. (a) Magnetization (M) versus temperature (T) plots measured in applied fields of (a) $H = 100$ Oe, (b) $H = 1$ kOe, (c) $H = 50$ kOe and (d) $H = 70$ kOe in the ZFC, FCC and FCW modes. FCC and FCW curves overlap at all temperatures. The $M_{ZFC}(T)$ and $M_{FC}(T)$ curves show bifurcation below T_N . The bifurcation also persists above T_N at least upto 150 K in the applied fields of 100 Oe. The inset in Fig. (a) shows the magnified view of ZFC and FCW curve above T_N in applied field of 100 Oe. The inset in Fig. (b) shows $\Delta M = M_{FC} - M_{ZFC}$ in fields of $H = 100$ Oe and 1 kOe. In applied fields of 50 kOe and 70 kOe $M_{ZFC}(T)$ and $M_{FC}(T)$ curves show a sudden and discontinuous fall in magnetization at T_N . $M_{ZFC}(T)$ and $M_{FC}(T)$ bifurcate below temperature $T_{irr} < T_N$ (see Figs. c and d).

Fig. 2(a) shows the temperature dependence of magnetization (M) in UO_2 measured at an applied field of $H = 100$ Oe in the zero field cooled (ZFC) warming, field cooled cooling (FCC) and field cooled warming (FCW) modes. In ZFC mode the measuring field $H = 100$ Oe is applied after cooling the sample to the lowest temperature (here 2 K) of measurement in zero external field. ZFC magnetization (M_{ZFC}) is then measured while warming the sample. After reaching the highest temperature (room temperature) of measurement the sample is subsequently cooled back to 2 K in same field while measuring the FCC magnetization (M_{FCC}). After FCC measurements the FCW magnetization (M_{FCW}) is measured while by warming the sample again gradually to room temperature in the same field. Temperature variation of magnetization in the high temperature regime in all the modes (ZFC, FCC and FCW) indicate the presence of

magnetic moment in UO_2 , which is in line with the Mott insulator status of the sample. Below $T = 50$ K, M tends to flatten while the temperature is further reduced and then M changes abruptly around $T_N = 30.6$ K. This temperature matches well with the reported temperature where UO_2 supposedly undergoes a phase transition to a complex antiferromagnetic state [12]. Figure 2(a) highlights the presence of a very distinct thermomagnetic irreversibility i.e. $M_{ZFC}(T) \neq M_{FC}(T)$ in the antiferromagnetic state. Such thermomagnetic irreversibility is not expected in any standard antiferromagnet [23], and to the best of our knowledge has not been reported earlier for UO_2 . $M_{FCC}(T)$ and $M_{FCW}(T)$ curves overlap at all temperatures of measurement and now onwards we will designate the field cooled magnetization as M_{FC} . Interestingly in an expanded scale (see the inset of Fig. 2(a)) one can see that the $M_{ZFC}(T)$ and $M_{FC}(T)$ curves actually start to bifurcate below $T = 150$ K, which is well over T_N and nearly equal to $5T_N$; the bifurcation gradually increases with decrease in temperature. The bifurcation between the $M_{ZFC}(T)$ and $M_{FC}(T)$ curves below the antiferromagnetic transition temperature T_N is much larger than the bifurcation above T_N . Just below the transition temperature, $M_{ZFC}(T)$ curve starts to rise sharply with increase in temperature, which is followed by a rapid fall resulting into a narrow peak around $T = 29$ K. Below about $T = 10$ K, $M_{ZFC}(T)$ curve increases slowly with decreasing temperature. All these features are not typical of a collinear antiferromagnet. Field cooled magnetization $M_{FC}(T)$ on the other hand rises sharply with decrease in temperature below T_N and tends to saturate below $T = 15$ K. Such a sharp rise in magnetization followed by a tendency towards saturation is not expected in the case of a collinear AFM state and is usually a characteristic feature of a ferromagnetic state. This kind of behaviour possibly arises due to non-collinear spin ordering within the AFM state of UO_2 , which results into weak ferromagnetic response below T_N . It may be noted here that, although the antiferromagnetic transition in UO_2 is reported to be first order in nature, $M_{FCC}(T)$ and $M_{FCW}(T)$ do not show any thermal hysteresis across T_N . It means that the supercooling and superheating phenomena, which are usually observed across a first order phase transition in many systems [24, 25], are absent across the antiferromagnetic transition in UO_2 .

Fig. 2(b) presents the results of the magnetization measurements as a function of temperature carried out in an applied magnetic field of $H = 1$ kOe. M_{ZFC} , M_{FCC} and M_{FCW} curves appear to be qualitatively similar to those obtained at $H = 100$ Oe. However, there are important differences, which are noted below:

- (i) The difference between M_{ZFC} and M_{FC} curves i.e. the thermomagnetic irreversibility above T_N is completely erased.
- (ii) The thermomagnetic irreversibility below T_N increases by a large extent than that at $H = 100$ Oe. The value of $\Delta M = M_{FCW} - M_{ZFC}$ at $H = 100$ and 1 kOe is shown in the inset of Fig. 2(b).
- (iii) Bifurcation of M_{ZFC} and M_{FC} curves starts just below T_N and this temperature does not seem to change with increase in applied magnetic field from 100 Oe to 1 kOe.

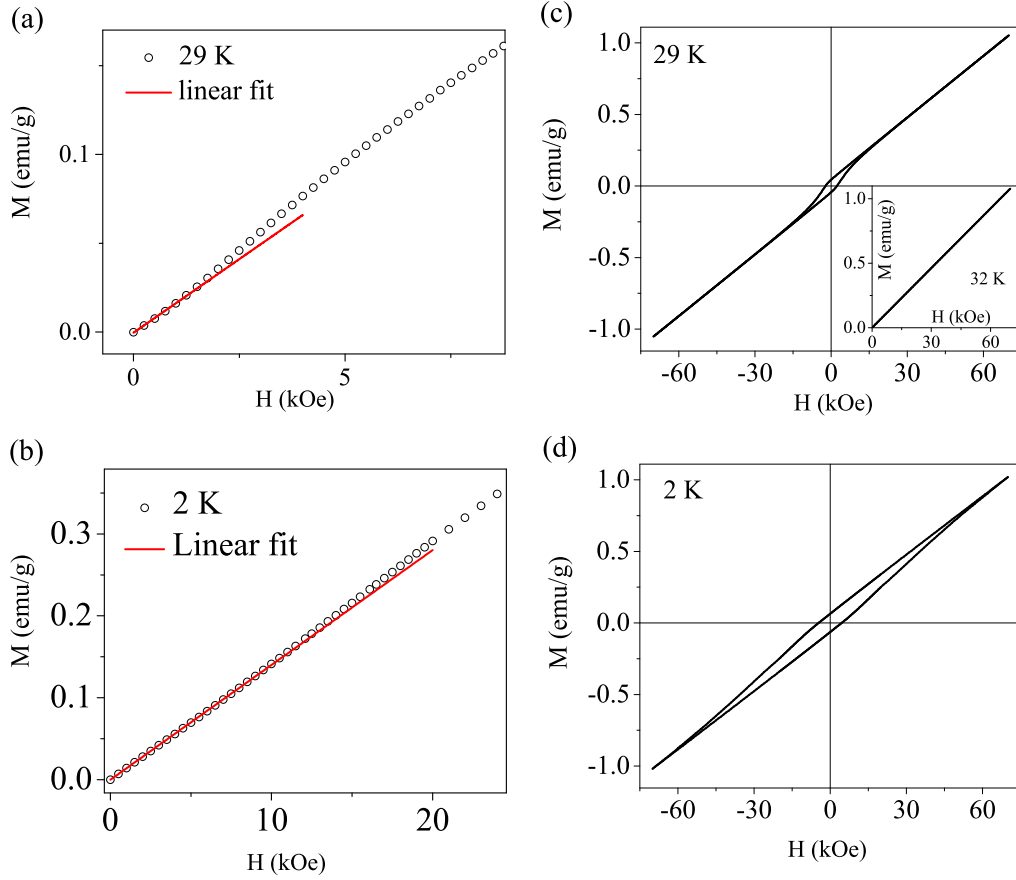


Figure 3. Isothermal field (H) variation of magnetization (M) in the antiferromagnetic regime at $T = 29$ K and 2 K: (a) and (b) show the virgin curves at $T = 29$ and 2 K near origin. $M(H)$ in the low field region is fitted and extrapolated to show the change in slope in the virgin $M-H$ curve. (c) and (d) show isothermal $M-H$ loops at $T = 29$ and 2 K. In the Inset of (c) $M-H$ curve at $T = 32$ K has been shown only in the first quadrant.

(iv) The low temperature increase in M_{ZFC} is more pronounced.

Thermomagnetic irreversibility is a characteristic feature of spin glass or cluster glass systems, where it arises due to freezing of spins or magnetic moments originating from the competing magnetic interactions and associated frustration [26, 27]. Thermomagnetic irreversibility is also observed in ferromagnets, which is associated with domain wall pinning [28]. Even some antiferromagnets with ThCr_2Si_2 structure exhibits thermomagnetic irreversibility, which was attributed to the stacking faults in those compounds with layered structures [29]. However, in all these magnetic systems the thermomagnetic irreversibility gets suppressed with increase in the applied magnetic field. This is in contrast with the observed increase in thermomagnetic irreversibility in UO_2 with the increase in applied fields from 100 Oe to 1 kOe. Such behaviour in UO_2 , however, changes in the region of high applied fields. Fig.2(c) and 2(d) present the temperature dependence of magnetization at $H = 50$ kOe and 70 kOe measured in ZFC, FCC and FCW modes. In this case the thermomagnetic

irreversibility as well as T_{irr} get reduced as the applied magnetic field is increased from 50 kOe to 70 kOe, whereas the antiferromagnetic transition temperature T_N remains largely unaffected. It may also be noted that the thermomagnetic irreversibility in the paramagnetic regime is totally absent in this high applied field regime.

From the results discussed above it is clear that magnetic response in low applied magnetic fields in both ZFC and FC states below T_N in UO_2 is distinctly different from that at high applied magnetic fields. More evidences in this direction emerge if one looks carefully to the temperature dependence of high field magnetization. As the UO_2 sample is cooled from high temperature, magnetization increases and tends to saturate around 35 K. However, just above T_N , magnetization decreases by a small amount, resulting into a small hump prior to T_N . The magnetic response at T_N , and also at low temperatures, change drastically both in the ZFC and FC states, as compared to magnetic behavior at low fields, shown in Fig. 2(a) and 2(b). At $H = 50$ kOe, both the $M_{ZFC}(T)$ and $M_{FC}(T)$ curves undergo an abrupt and discontinuous fall at T_N , which is immediately followed by a small rise in magnetization with decrease in temperature. Then, they show a relatively flat region over a temperature region of 28-22 K. In the lower temperature region, the M_{ZFC} and M_{FCC} curves bifurcate: the M_{ZFC} curve starts to decrease, whereas the M_{FCC} curve slowly increases. Note that, the M_{ZFC} also shows an additional shallow dip around $T_d = 15$ K. Note that, the bifurcation between $M_{ZFC}(T)$ and $M_{FC}(T)$ curves appears only below a temperature T_{irr} (see Fig. 2(c)), which is lower than the transition temperature T_N . At $H = 70$ kOe, magnetization shows larger drop at T_N and all the three curves gradually decrease with further decrease in temperature (see Fig. 2(d)). Below T_{irr} , the M_{ZFC} curve continues to decrease, whereas the M_{FCC}/M_{FCW} curve increases. This is in clear contrast to the temperature dependence of magnetization obtained in applied magnetic fields of 100 Oe and 1 kOe (see Fig. 2(a) and 2(b)).

To investigate further on the antiferromagnetic state in UO_2 , we present in Fig. 3 the isothermal $M - H$ curves at $T = 29$ and 2 K measured starting from the ZFC state. Here, the sample is initially cooled to the temperature of measurement in the absence of any external field. Then M is measured while increasing H isothermally to 70 kOe to record initial (virgin) curve, which is shown in Figs. 3(a) and 3(b) for $T = 29$ and 2 K, respectively. After recording the virgin curve, M is measured while varying H between ± 70 kOe to record the envelope curves, which are shown in Figs. 3(c) and 3(d). The virgin curves at both temperature lie within the envelope curves. Note that, at $T = 29$ K, the $M - H$ curve shows a small change in the slope above $H_a = 1.2$ kOe and continues to increase at higher field up to the highest applied field of $H = 70$ kOe. Whereas, the virgin $M - H$ curve at $T = 2$ K deviates from linearity above $H_a = 15$ kOe. The envelope $M - H$ curve at $T = 29$ K shows a small hysteresis with a coercive field of around $H_C = 2.2$ kOe, which increases to 4.5 kOe at 2 K. The $M - H$ curves do not show any tendency of saturation till $H = 70$ kOe. The nonsaturating $M - H$ curve highlights the antiferromagnetic state but the presence of hysteresis is rather unexpected in AFM state. At further lower temperature, both coercive field and remanant magnetization further increase as evident from the $M - H$ curve at $T = 2$ K.

This change in the slope of $M - H$ curves above $H = H_a$, may indicate some sort of field induced transition of the zero field cooled AFM state.

The increase in the difference between $M_{ZFC}(T)$ and $M_{FC}(T)$ with magnetic applied magnetic field is one of the important signatures of a kinetically arrested first order transitions[25, 31, 32, 33, 34]. In this case, the dynamics of a first order phase transition gets arrested in a $H - T$ window. The difference between $M_{ZFC}(T)$ and $M_{FC}(T)$ increases because cooling in different magnetic fields produce different volume fractions of the high and low temperature magnetic phases. As stated earlier, the transition in UO_2 is first order in nature, and like a kinetically arrested system thermomagnetic irreversibility in the low field regime increases with the applied magnetic field. In this context, the $M - H$ curves shown in Fig. 3, can be rationalized in the following manner: the ZFC state undergoes a field induced transition above a critical field H_a , as observed from the change in slope. However, in the field decreasing cycle, the reverse transition is not observed, so that the magnetic state induced by applied magnetic field persists during the entire envelope curve and gives rise to hysteresis loop. Such behaviour has been reported in the literature in the cases of kinetic arrest of first order phase transition in various magnetic systems, where the zero field cooled state may be either equilibrium low- T phase, or the kinetically arrested high- T phase, depending on the nature of the ground state [35, 34]. Now, after zero field cooling, in the first case, when magnetic field is increased, above certain field, the equilibrium phase undergoes a field induced transition to the high- T phase as the superheating band is crossed [32, 34, 35]. On the other hand, in the second case, the kinetically arrested state devitrify into the equilibrium low- T phase while increasing the field. In either cases, the envelope curve does not show the reverse transition.

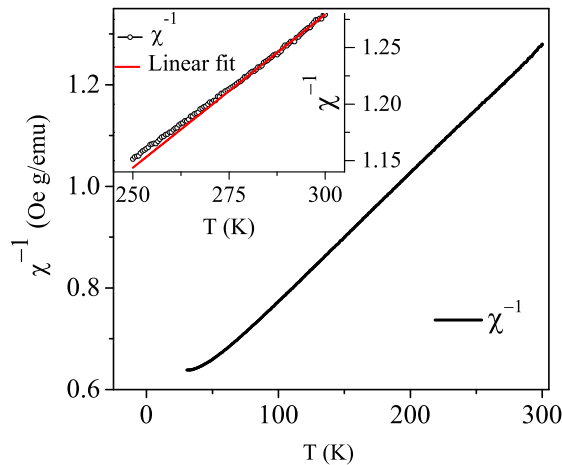


Figure 4. χ^{-1} versus T data measured at $H = 100$ Oe in the ZFC mode. The inset shows the CW law fitting above 280 K.

The unusual dependence of magnetization on temperature and the finite difference between $M_{ZFC}(T)$ and $M_{FC}(T)$ curves much above T_N clearly highlight an unconventional paramagnetic state at high temperatures. Therefore, to further

understand the magnetic property of UO_2 at high temperatures, χ^{-1} versus T at $H = 100$ Oe measured in ZFC mode is plotted in Fig. 4. The χ^{-1} versus T data appears to be grossly linear in the temperature range from $T = 300$ K to 70 K. We tried to fit the results in this temperature regime by using Curie-Weiss (CW) law, given by $\chi = \frac{C}{T+T_0}$, where $C = \frac{N\mu_{eff}^2}{3k_B} = \frac{Ng^2J(J+1)}{3k_B}$. However, when looked carefully, the CW law does not fit the experimental data in the entire temperature regime. In fact, it deviates from linearity below around $T = 280$ K (see the inset of Fig. 4). The effective magnetic moment μ_{eff} obtained to be $2.82 \mu_B/\text{f.u.}$, which is smaller than the expected value of $3.57 \mu_B/\text{f.u.}$ for $J = 4$ ($L = 5$ and $S = 1$). However, it matches extremely well with value of effective moment expected for the threefold degenerate ground state in UO_2 in a cubic crystal field [12]. T_0 is obtained to be around 171 K, which is around 5.6 times higher than the transition temperature. The deviation of the susceptibility from CW law, the presence of irreversibility much above T_N , higher value of T_0 than T_N are interesting. There exist some earlier reports of the unusual characteristics above T_N [8]. In inelastic neutron scattering experiments, magnetic inelastic response has been observed above T_N up to as high as $T = 200$ K [20]. It has been suggested that the coherent motion of the neighbouring oxygen cages produces uncorrelated 1-k type dynamical JT distortion in the paramagnetic state of UO_2 [20]. With the lowering in temperature correlation builds up and a static 3-k type distortion condenses at T_N . The tendency of M to saturate as T_N is approached during cooling, the deviation from the CW law, existence of bifurcation between the ZFC and FC curves highlight the unusual paramagnetic state at high temperature, which may arise due to short range 1-k type dynamic JT distortion.

4. Conclusion

Summarizing, we can say from the results of temperature and magnetic field dependent studies of dc magnetization that the low temperature antiferromagnetic state in UO_2 is non-trivial in nature and is accompanied with large thermomagnetic irreversibility. The field cooled magnetization $M_{FC}(T)$ measured in low fields of 100 Oe and 1 kOe indicates the presence of ferromagnetic character in UO_2 . This inference is further corroborated by the presence of hysteresis in isothermal field variation of magnetization alongwith appreciable coercive field. The nature of the thermomagnetic irreversibility changes in the presence of high applied magnetic field. In the low magnetic field region the thermomagnetic irreversibility increases with the increase in applied field, which can be rationalized in terms of the kinetic arrest of magnetic field induced first order phase transition. The thermomagnetic irreversibility in the high magnetic field regime decreases with the increase in applied field. Prima facie this behaviour is quite similar to that observed in some ferro and antiferromagnets, where it was attributed to the hindrance in domain wall motion. Furthermore the paramagnetic state in UO_2 is also unusual with a deviation of Curie-Weiss law and the presence of thermomagnetic irreversibility in the temperature region much above T_N . These results indicate the

existence of some short range magnetic correlations well inside the paramagnetic region of UO_2 . Overall the results of our present study are expected to stimulate further microscopic measurements involving neutron scattering and muon spin rotation (μSR) measurements to find out the exact microscopic nature of magnetic states in various magnetic field (H) - temperature (T) regime of UO_2 .

5. Acknowledgment

We acknowledge Dr. Vinay Kumar of Bhabha Atomic Research Centre, Trombay for providing us with powdered UO_2 sample and Dr. A. Sagdeo and Dr. A. K. Sinha of Raja Ramanna Centre for Advanced Technology, Indore for help in X-ray diffraction measurement. S B Roy acknowledges financial support from Department of Atomic Energy, India in the form of Raja Ramanna Fellowship. Sudip Pal and S B Roy thank Dr. A. J. Pal, Director, UGC-DAE CSR and Dr. D. M. Phase, Centre Director, UGC-DAE CSR, Indore Centre for support and encouragement.

6. References:

- [1] Quan Yin and Sergey Y. Savrasov, Phys. Rev. Lett **100**, 225504 (2008).
- [2] S. -W. Yu et al, Phys. Rev. B **83**, 165102 (2011).
- [3] J. Schoenes, J. Appl. Phys. **49** 1463 (1978).
- [4] S. B. Roy, *Physics of Mott insulator: Physics and applications*, IOP Publishing (2019).
- [5] Jack Leland Daniel, J. Matolich, H. W. Deem, *Thermal conductivity of UO_2* , Hanford atomic products operation (1962).
- [6] J. H. Harding and D. G. Martin, J. Nucl. Mater. **166**, 223 (1989).
- [7] P.G.Lucuta, H.J. Matzke, I.J.Hastings, J. Nucl. Mater. **232**, 166 (1996).
- [8] K. Gofryk et al, Nature Communication 5:4551 (2014).
- [9] M. Jaime et al, Nature Communication 8: 99 (2017).
- [10] P. Burlet, J. Rossat-Mignod, S. Quezel, O. Vogt, J.C. Spirlet, and J. Rebizant, J. Less-Common Met. **121**, 121 (1986).
- [11] Ogden G. Brandt and Charles T. Walker, Phys. Rev. Lett **18**, 11 (1967).
- [12] K. Ikushima et al, Phys. Rev. B **63** 104404 (2001).
- [13] H.U. Rahman and W.A. Runciman, J. Phys. Chem. Solids **27**, 1833 (1966); **30**, 2497 (1969); H.U. Rahman, Physica (Amsterdam) , 511 (1970).
- [14] S.J. Allen, Phys. Rev. **166**, 530 (1968); **167**, 492 (1968).
- [15] S. B. Wilkins, R. Caciuffo, C. Detlefs, J. Rebizant, E. Colineau, F. Wastin, and G. H. Lander, Phys. Rev. B **73**, 060406(R) (2006).
- [16] R. Caciuffo, G. van der Laan, L. Simonelli, T. Vitova, C. Mazzoli, M. A. Denecke, and G. H. Lander, Phys. Rev. B **81**, 195104, (2010).
- [17] Leonid V. Pourovskii and Sergii Khmelevskiy, Phys. Rev. B **99** 094439 (2019).
- [18] J. Faber, G. Lander and B. Cooper, Phys. Rev. Lett. **35**, 1770 (1975).
- [19] J. Faber and G. Lander, Phys. Rev. B **14**, 1151 (1976)
- [20] R. Caciuffo, G. Amoretti, P. Santini, G. H. Lander, J. Kulda, and P. de V. Du Plessis, Phys. Rev. B **59**, 13 892 (1999).
- [21] R. Caciuffo, P. Santini, S. Carretta, G. Amoretti, A. Hiess, N. Magnani, L.-P. Regnault, and G. H. Lander, Phys. Rev. B **84**, 104409 (2011).
- [22] K. Teske, H. Ullmann, and D. Rettig, J. Nucl. Mater. **116**, 260 (1983).
- [23] S. J. Blundell, Magnetism in Condensed Matter (Oxford University Press, 2001).

- [24] S. B. Roy, G. K. Perkins, M. K. Chattopadhyay, A. K. Nigam, K. J. S. Sokhey, P. Chaddah, A. D. Caplin and L. F. Cohen, *Phys. Rev. Lett.*, **92** 147203 (2004).
- [25] S. B. Roy, *J. Phys.: Condens. Matter* **25** 183201 (2013).
- [26] J. A. Mydosh, *Rep. Prog. Phys.* **78**, 052501 (2015).
- [27] Sudip Pal, Kranti Kumar, A. Banerjee, S. B. Roy and A. K. Nigam, *J. Phys.: Condens. Matter* **33** (2021) 025801 (2021) and references therein.
- [28] S.B. Roy, A.K. Pradhan, P. Chaddah and B.R. Coles, *Solid St. Commun.* **99** 563 (1996).
- [29] S. B. Roy, A.K. Pradhan and P. Chaddah, *J. Phys.: Condens. Matter* **6** 5155 (1994).
- [30] S.B. Roy, A.K. Pradhan, P. Chaddah and E. V. Sampathkumaran, *J. Phys.: Condens. Matter* **9** 2465 (1997).
- [31] M. K. Chattopadhyay, S. B. Roy, and P. Chaddah, *Phys. Rev. B* **72**, 180401(R) (2005).
- [32] A. Banerjee, K. Mukherjee, Kranti Kumar, and P. Chaddah, *Phys. Rev. B* **74**, 224445 (2006).
- [33] S. B. Roy and M. K. Chattopadhyay, *Phys. Rev. B* **79**, 052407 (2009).
- [34] P. Chaddah, *First Order Phase Transitions of Magnetic Materials* (Taylor and Francis, 2017).
- [35] Kranti Kumar et al, *Phys. Rev. B* **73** 184435 (2006).